Effects of Target Trajectory Bandwidth on Manual Control Behavior in Pursuit and Preview Tracking

Van Der El, Kasper; Pool, Daan M.; Van Paassen, Marinus M.; Mulder, Max

DOI
10.1109/THMS.2019.2947577

Publication date
2020

Document Version
Accepted author manuscript

Published in
IEEE Transactions on Human-Machine Systems

Citation (APA)
Van Der El, K., Pool, D. M., Van Paassen, M. M., & Mulder, M. (2020). Effects of Target Trajectory Bandwidth on Manual Control Behavior in Pursuit and Preview Tracking. *IEEE Transactions on Human-Machine Systems*, *50*(1), 68-78. Article 8897675. https://doi.org/10.1109/THMS.2019.2947577

Effects of Target Trajectory Bandwidth on Manual Control Behavior in Pursuit and Preview Tracking

Kasper van der El, *Member, IEEE*, Daan M. Pool, *Member, IEEE*, Marinus (René) M. van Paassen, *Senior Member, IEEE*, and Max Mulder, *Member, IEEE*

***Abstract*—The 1960s crossover model is widely applied to quantitatively predict a human controller's (HC's) manual control behavior. Unfortunately, the theory captures only compensatory tracking behavior and, as such, a limited range of real-world manual control tasks. This article finalizes recent advances in manual control theory toward more general pursuit and preview tracking tasks. It is quantified how HCs adapt their control behavior to a final crucial task variable: the target trajectory bandwidth. Beneficial adaptation strategies are first explored offline with computer simulations, using an extended crossover model theory for pursuit and preview tracking. The predictions are then verified with data from a human-in-the-loop experiment, in which participants tracked a target trajectory with bandwidths of 1.5, 2.5, and 4 rad/s, using compensatory, as well as pursuit and preview displays. In stark contrast to the crossover regression found in compensatory tasks, humans attenuate only their feedforward response when tracking higher-bandwidth trajectories in pursuit tasks, while their behavior is generally invariant in preview tasks. A full quantitative theory is now available to predict HC manual control behavior in tracking tasks, which includes HC adaptation to all key task variables.**

***Index Terms*—Manual control, modeling, pursuit, preview, target trajectory bandwidth.**

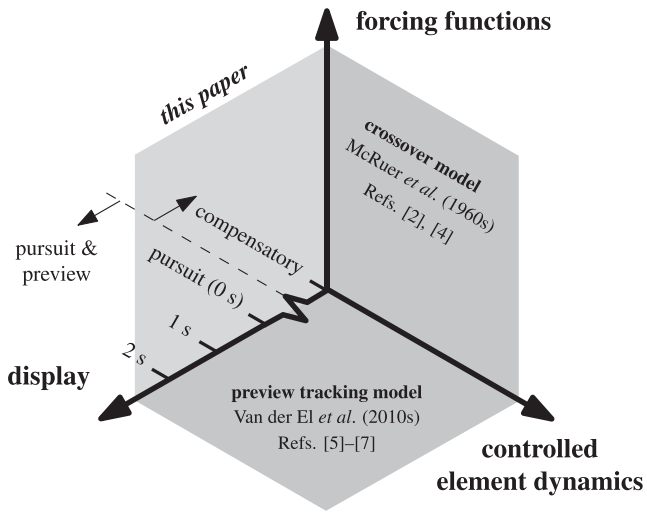

Fig. 1. Illustration of the task variables that evoke adaptations in manual control behavior, which have been quantified by the indicated literature.

I. Introduction

HUMANS exhibit highly adaptive behavior when manually controlling vehicles and devices [1]. The human controller's (HC's) versatility is currently not yet matched by automatic controllers, and can be a key argument for keeping humans in-the-loop in the near future. However, exactly these adaptive capabilities make it difficult to accurately predict HC behavior and its interaction with novel technologies. Three crucial task variables that are known to strongly affect HC behavior are the controlled element (CE) dynamics, the display configuration, and the forcing functions (target trajectory and disturbances) [2], [3], as illustrated in Fig. 1. Already in the 1960s, McRuer and his colleagues advanced a quantitative theory for human control behavior in compensatory tracking tasks [2], the *crossover model*, together with *verbal adjustment rules* for predicting HC adaptation to the task variables.

The crossover model is still widely used today to predict HC behavior, even though its applicability is limited, as only the human's *error feedback* response is captured. HCs in practice often rely on feedforward control for adequate task performance, based on knowledge of the *target trajectory* [4]–[6]. This is known as pursuit control behavior when only the *current* target value is used, or preview control behavior when also the *future* trajectory is used. In our recent work [7], we proposed an extension to the crossover model theory, to also capture HC behavior in the more relevant pursuit and preview tracking tasks. This extended model allows for rationalizing and predicting the HC's feedforward response, and has already been used to study HC behavior *adaptations* in tasks with various CE dynamics and preview times in [8] and [9].

One crucial link is still missing in the theory, as illustrated in Fig. 1: HC adaptation to the forcing function characteristics in pursuit and preview tracking tasks. In compensatory tracking tasks, HCs particularly adapt their behavior to the target trajectory *bandwidth*. HCs follow higher-bandwidth target trajectories with increasing control gains to keep the open-loop crossover frequency well above the input bandwidth [10]. Ultimately, however, an increased control gain leads to instability, and HCs are forced to strongly reduce their control gain in very high-bandwidth target-tracking tasks, which manifests as *crossover-regression* [10]–[13]. The crossover model has been

Manuscript received November 29, 2018; revised June 24, 2019; accepted September 22, 2019. Date of publication November 13, 2019; date of current version January 14, 2020. This article was recommended by Associate Editor R. A. Hess. *(Corresponding author: Kasper van der El.)*

The authors are with the Control and Simulation Section, Faculty of Aerospace Engineering, Delft University of Technology, 2629 HS Delft, The Netherlands (e-mail: k.vanderel@tudelft.nl; d.m.pool@tudelft.nl; m.m.vanpaassen@tudelft.nl; m.mulder@tudelft.nl).

Digital Object Identifier 10.1109/THMS.2019.2947577

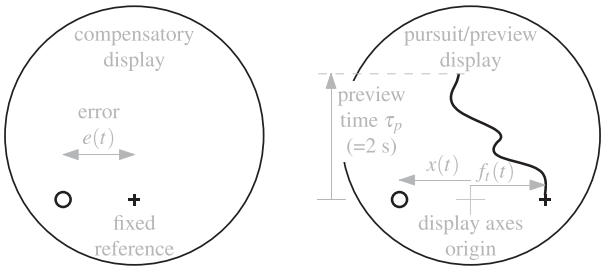

Fig. 2. Experimental compensatory and pursuit/preview displays; only the black markers were visible to the participants (note, $\tau_p = 0$ s in pursuit tasks).

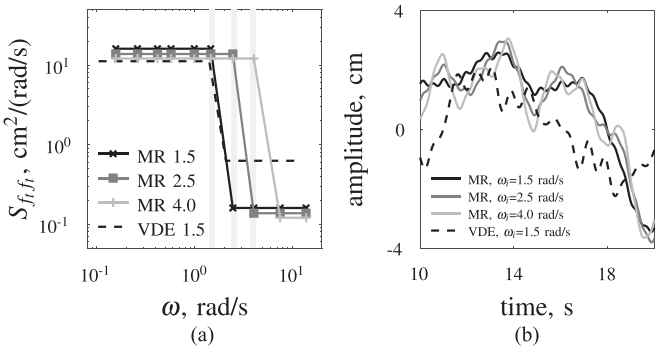

Fig. 3. Target signal spectra (a) and time traces (b), used by McRuer *et al.* [2] (MR) and Van der El *et al.* [7]–[9] (VDE); vertical lines and numbers (e.g., 1.5) indicate the bandwidth ω_i in rad/s, power $\sigma^2_{f_t} = 1.61$ cm^2 (=0.25 in.^{2}).

instrumental for our understanding of these contradictory behavior adaptations [10]–[13], but, due to the lack of a feedforward model, cannot fully explain HC adaptation in pursuit [4], [14] and preview [15], [16] tracking tasks.

This article attempts to complete the theory of HC manual control in pursuit and preview tracking tasks, by investigating how HCs adapt their control behavior to the bandwidth of the target trajectory. Beneficial adaptation strategies are first explored offline (in Sections II and III), using the HC model from [7]. Predicted behavior adaptations are then verified with data from a human-in-the-loop experiment (in Sections IV and V), in which participants performed a double-integrator tracking task with compensatory, pursuit, and preview displays, and three target-trajectory bandwidths (1.5, 2.5, and 4 rad/s). The HC model for pursuit and preview tracking is fit to the measurement data, to quantify how HCs adapt their control behavior to the target bandwidth, providing insight beyond the overt performance effects that are often provided in the literature [4], [14]–[16]. This paper ends with a discussion and the main conclusions in Sections VI and VII.

II. Control Task

A. Manual Tracking

Fig. 2 shows two *tracking* displays. HCs are to minimize the tracking error $e(t) = f_t(t) - x(t)$ between a target trajectory $f_t(t)$ and the corresponding CE output variable $x(t)$. In compensatory tasks only the error $e(t)$ is available, see Fig. 2 for an example compensatory display. In addition to the tracking error, pursuit tasks explicitly show both the target and the CE output, for example, through two separate markers on a display (see Fig. 2). The future target trajectory ahead may also be visible up to the preview time τ_p; in pursuit tasks $\tau_p = 0$ s by definition, in preview tasks $\tau_p > 0$ s. Additionally, disturbances $f_d(t)$ may perturb the CE, yielding a combined target-tracking and disturbance-rejection task.

B. Target Signal Power and Bandwidth

To characterize the target signal that an HC is to follow, researchers typically report the signal's *power* and *bandwidth* [4], [10], [16], [17]. The power (or variance) is given by $\sigma^2_{f_t} = \frac{1}{\pi}\int_0^\infty S_{f_t f_t}(j\omega)\,\mathrm{d}\omega$, with $S_{f_t f_t}(j\omega)$ the target signal's power-spectral density function [18]. The bandwidth ω_i is defined as the highest frequency at which the target signal has significant power. In their landmark compensatory tracking experiment, McRuer *et al.* [10] systematically increased the bandwidth from 1.5 to 2.5 and 4 rad/s, yielding an increasingly demanding task. The target signals used by McRuer *et al.* [10], which are shown in Fig. 3, were all the sum of ten sinusoids[1]

$$f_t(t) = \sum_{k=1}^{10} A_t[k]\sin(\omega_t[k]t + \phi_t[k]) \tag{1}$$

with frequency $\omega_t[k]$, amplitude $A_t[k]$, and phase $\phi_t[k]$ of the kth sinusoid. At frequencies beyond the bandwidth ω_i, the vertical gray lines in Fig. 3(a), the amplitudes are strongly attenuated, but still nonzero to allow for measuring the HC's dynamics over the full frequency range of interest [17].

C. Other Target Signal Characteristics

To tie in with previous work on compensatory tracking [2], [11], this article also focuses on the effects of bandwidth. However, it is important to note that bandwidth may not be the only parameter to which HCs adapt their behavior [18]. Apparently small changes in the number of sinusoids, frequencies, amplitudes, and phases can also severely affect the signal's time-domain appearance, and hence the HC's behavior.

For example, Fig. 3 also shows the 1.5 rad/s bandwidth target signal ("VDE") that was used in recent pursuit and preview tracking experiments [7]–[9]. This signal's spectrum matches McRuer's 1.5 rad/s bandwidth signal fairly well and has equal power, but is composed of 20 sinusoids (instead of 10) and the high-frequency amplitudes are higher (to avoid HCs from ignoring these sine components, which are explicitly visible in preview tasks). The time traces of these two signals are very different, see Fig. 3(b); they may therefore still evoke different HC behavior, despite their equal power and bandwidth.

[1]Opposed to sums-of-sinusoid signals, low-pass filtered white noise can—and has been—used in human-in-the-loop experiments [18]. The advantage of sums-of-sinusoids is that they can serve as instrumental variables for estimating HC control dynamics with frequency-domain system identification techniques [10], [18]–[20]. However, enough sine components must be included for the signal to be random-appearing, or HCs will exploit predictable patterns through "precognitive" open-loop feedforward control [5], [21]–[24].

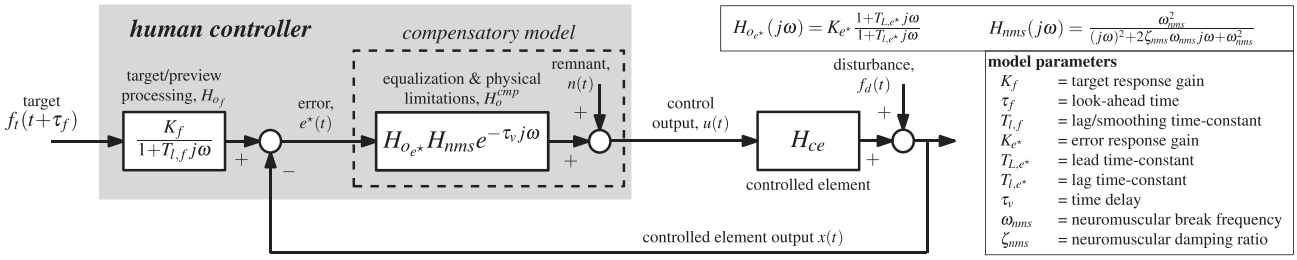

Fig. 4. HC model for pursuit and preview tracking tasks from [7], which extends the crossover model for compensatory tracking by McRuer *et al.* [2], [10]. The "near-viewpoint" response that humans occasionally mechanize in preview tasks is omitted for simplicity; this response captures the relatively weak and high-frequency target-tracking behavior and is difficult to predict (see [8] for an elaborate discussion on the near-viewpoint response).

Moreover, measuring HC adaptation to bandwidth in isolation is in fact impossible, as the amplitudes, bandwidth, and power are interdependent. This is visible in the three signals from McRuer *et al.* [10]: constructing signals with different bandwidths, yet equal power, required adapting the amplitudes of *all* the individual sine-components [see Fig. 3(a)]. In conclusion, despite the focus on the effects of bandwidth, here and in the literature, various underlying parameters affect the appearance of a target signal, and can thus—subtly or obviously—affect HC behavior [18].

D. HC Model

Fig. 4 shows the quasi-linear HC model for manual preview tracking, adapted from [7]. As opposed to the more common model structure with parallel error minimization and feedforward responses (see [4], [16], [25], among others), this model combines a target trajectory *prefilter* with error minimization. While both models are equivalent and can capture the HC dynamics equally well, the prefilter model enables a more intuitive interpretation of HC adaptation in preview tasks, see [8] and [9]. In the prefilter, any required lead equalization is generated by varying the look-ahead time τ_f, in contrast to inverting the CE dynamics in a parallel feedforward response.

In Fig. 4, the HC control outputs $u(t)$ are based on the portion of the target trajectory up to τ_f s ahead, which is weighted (through K_f) and smoothed (through $T_{l,f}$) before being compared to the CE output to yield an "internal" error $e^\star(t)$. The total target prefilter dynamics are: $H_{o_f}(j\omega) = K_f e^{\tau_f j\omega}(1+T_{l,f}j\omega)^{-1}$. In pursuit tasks, the lack of preview ($\tau_p = 0$ s) prevents HCs from using the trajectory ahead for control, such that $\tau_f = T_{l,f} = 0$ s. HCs can still respond to both the target and the CE output, prioritizing either one response by adapting the weighing gain K_f. The model can also capture HC behavior in compensatory tracking tasks; by setting $K_f = 1$ and $\tau_f = T_{l,f} = 0$ s, it follows that $e^\star(t) = e(t)$, such that the modeled HC responds to the true error.

Regardless of the display configuration, HCs select an error (e or $e^\star$) to use for compensatory-like control. The error response dynamics are $H_o^{\text{cmp}}(j\omega) = H_{o_{e^\star}}(j\omega)H_{\text{nms}}(j\omega)e^{-\tau_v j\omega}$, with equalization dynamics $H_{o_{e^\star}}(j\omega)$, neuromuscular activation dynamics $H_{\text{nms}}(j\omega)$, and a time delay τ_v. The equalization is equivalent to McRuer's simplified precision model [2], and mainly depends on the CE dynamics [8].

III. Offline Analysis

A. Performance Measures as Motivation for Adaptation

HC control behavior, and HCs' adaptation thereof, is typically motivated by optimizing task performance, while ensuring sufficient stability margins and avoiding excessive control effort [2]. A measure for performance is the variance of the tracking error $\sigma_e^2 = \frac{1}{\pi}\int_0^\infty S_{ee}(j\omega)\,\mathrm{d}\omega$, with $S_{ee}(j\omega)$ the power-spectral density of the error signal [18]:

$$S_{ee}(j\omega) = |H_{f_t,e}(j\omega)|^2 S_{f_t f_t}(j\omega) + |H_{f_d,e}(j\omega)|^2 S_{f_d f_d}(j\omega) + |H_{n,e}(j\omega)|^2 S_{nn}(j\omega). \quad (2)$$

The input-to-error transfer functions $H_{f_t,e}(j\omega)$, $H_{f_d,e}(j\omega)$, and $H_{n,e}(j\omega)$ reflect the HC's proficiency in suppressing errors due to the target $S_{f_t f_t}(j\omega)$, disturbance $S_{f_d f_d}(j\omega)$, and remnant $S_{nn}(j\omega)$ signals, respectively. As the target signal is explicitly visible in the considered pursuit and preview tracking tasks, the target-to-error dynamics $H_{f_t,e}(j\omega)$ are of primary interest. For a sum-of-sinusoids target with frequencies ω_t, the target-to-error dynamics are defined as $H_{f_t,e}(j\omega_t) = \frac{E(j\omega_t)}{F_t(j\omega_t)}$ [8], [11], with E and F_t the discrete Fourier transforms of the error and target signals, respectively. After substituting $E(j\omega_t) = F_t(j\omega_t) - X(j\omega_t)$, the following expression can be obtained using Fig. 4 [8]:

$$H_{f_t,e}(j\omega_t) = \frac{1 + H_{ce}(j\omega_t)H_o^{\text{cmp}}(j\omega_t)[1 - H_{o_f}(j\omega_t)]}{1 + H_{ce}(j\omega_t)H_o^{\text{cmp}}(j\omega_t)}. \quad (3)$$

Similar expressions can be obtained for $H_{f_d,e}(j\omega_d)$ and $H_{n,e}(j\omega)$ (see [2], [8], [14], [20] for details). HCs follow the target trajectory *perfectly*, with zero tracking errors, when $H_{f_t,e}(j\omega_t) = 0$; substitution in (3) then leads to the following expression for the "perfect" target prefilter dynamics:

$$H_{o_f}^P(j\omega_t) = 1 + \frac{1}{H_{ce}(j\omega_t)H_o^{\text{cmp}}(j\omega_t)}. \quad (4)$$

The $H_{ce}(j\omega)H_o^{\text{cmp}}(j\omega)$ term corresponds to the open-loop dynamics in compensatory tracking tasks, which typically resemble an integrator with a delay according to the crossover model [2]. Consequently, (4) shows that HCs must generate lead in the prefilter to track the target signal perfectly. Note that the model in Fig. 4 suggests that actual HCs do the exact opposite in preview tasks, namely target smoothing ($\frac{1}{1+T_{l,f}j\omega}$). The required

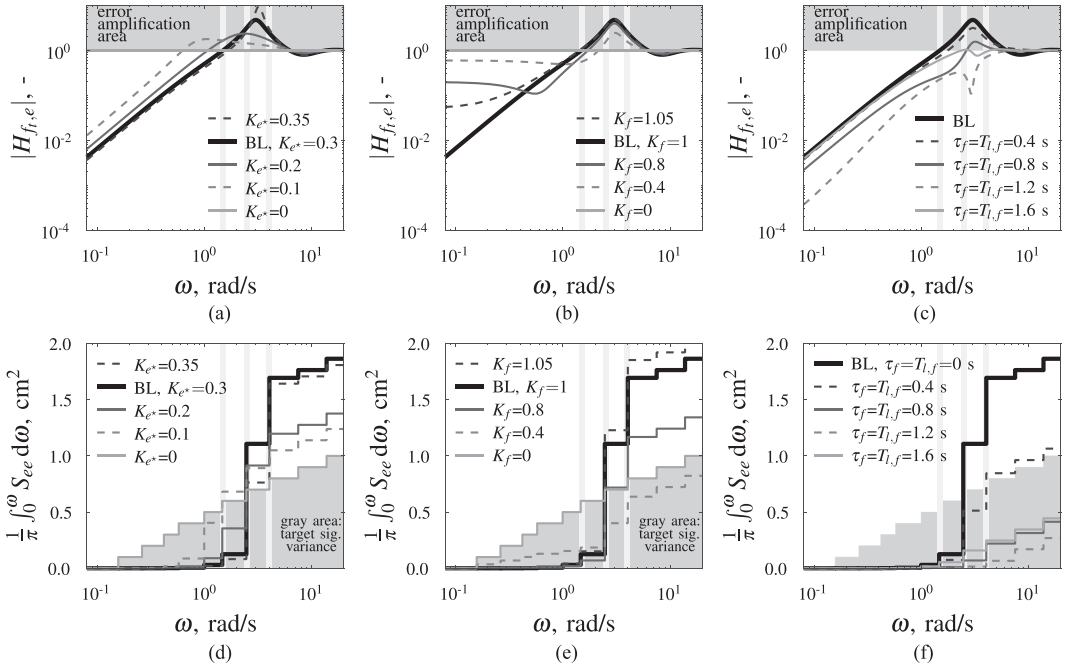

baseline (BL) model parameters, from [7]

H_{ce}	$\frac{5}{(j\omega)^2}$
$K_{e^\star}$, -	0.3
$T_{L,e^\star}$, s	1.5
$T_{l,e^\star}$, s	0
τ_v, s	0.28
ω_{nms}, rad/s	8.5
ζ_{nms}, -	0.45
K_f, -	1
$T_{l,f}$, s	0
τ_f, s	0

Fig. 5. Effects of model parameters on the target-to-error dynamics in a double integrator task for compensatory (a), pursuit (b), and preview (c) configurations, and the corresponding cumulative error for a sum-of-ten-sines target signal ($\sigma^2_{f_t} = 1$ cm^2) with equal amplitudes at all frequencies for compensatory (d), pursuit (e), and preview (f) configurations. Gray vertical lines are the three bandwidths tested by McRuer *et al.* [10].

lead is still achieved, although only in *phase*, by responding to the trajectory τ_f s ahead ($e^{\tau_f j\omega}$ term) [8].

Other common measures for performance (and stability) are the open-loop crossover frequency ω_c and phase margin ϕ_m [2], [8]. The target open-loop frequency-response function is $H_{ol,t}(j\omega_t) = H_{f_t,e}{}^{-1}(j\omega_t)$-1 [8], [20]. In manual control, target-tracking errors are generally low at frequencies below the crossover frequency, so for $\omega_t \ll \omega_{c,t}$ [2], [11].

B. Manual Control Adaptation in Compensatory Tasks

The magnitude of the target-to-error dynamics $|H_{f_t,e}(j\omega)|$ is shown for different sets of model parameters for a double integrator compensatory task in Fig. 5(a). A "baseline" (BL) HC model is shown with a thick black line, and is based on the average model parameters estimated from experimental data in [9]. At low frequencies, $|H_{f_t,e}(j\omega)| \ll 1$ for the BL model, so the tracking errors are small and the target signal is tracked well. However, due to the HC's response delay τ_v, $|H_{f_t,e}(j\omega)| > 1$ is seen between 1.5 and 6 rad/s, yielding errors that exceed the magnitude of the target signal and poor tracking performance.

From (2), it is clear that not only $|H_{f_t,e}(j\omega)|$, but also the target signal input spectrum $S_{f_t f_t}(j\omega)$ contributes directly to the tracking error. A target signal with $\omega_t < 1.5$ rad/s bandwidth [left gray vertical line in Fig. 5(a)] is tracked well with the BL HC behavior, as the tracking errors are suppressed at all these frequencies. However, higher frequencies in the target signal [e.g., 4 rad/s, see Fig. 5(a)] excite the error-amplification peak of $H_{f_t,e}(j\omega)$ and thus yield a strong decrease in tracking performance. By adapting their control behavior HCs can change the shape of $H_{f_t,e}(j\omega)$ to avoid amplifying the errors at frequencies where the target signal's power is concentrated. To do so, HCs typically adapt their response gain $K_{e^\star}$ and lead equalization $T_{L,e^\star}$, their response time delay τ_v, or the properties of their neuromuscular system (ω_{nms} or ζ_{nms}). Fig. 5(a) shows the effect of lowering the response gain $K_{e^\star}$: the error-amplification peak reduces, but also becomes wider.

Fig. 5(d) shows how each frequency contributes to the error. For a target signal of 1.5 rad/s bandwidth, the BL behavior ($K_{e^\star} = 0.3$) still provides superior performance (the thick black line is lowest at the left-most vertical gray line), but this same behavior yields a sharp increase in tracking error for signals of 2.5 rad/s bandwidth (at the middle vertical line). Higher-gain control provides better performance here [e.g., $K_{e^\star} = 0.35$ in Fig. 5(d)]. At 4 rad/s also the high-gain strategy leads to substantial tracking errors, and a severe reduction of the control gain (e.g., to $K_{e^\star} = 0.1$) is beneficial. Such a reduced control gain typically leads to regression of the open-loop crossover frequency to a value below the target signal bandwidth [2], [11]. Fig. 5(d) shows that reduced-gain control becomes superior to higher-gain control from around 4 rad/s and higher, which corresponds well to the input bandwidths at which crossover regression is reported throughout the literature for double-integrator CE dynamics tasks (between 3 and 4 rad/s [2], [10]–[12]).

C. Manual Control Adaptation in Pursuit and Preview Tasks

In pursuit tasks, HCs can additionally adapt their target response gain K_f to improve error suppression. Similar as reducing $K_{e^\star}$, a lower K_f leads to a reduced error-amplification peak, at the cost of inferior low-frequency tracking performance, see Fig. 5(b). When K_f is zero, the HC completely ignores the

target signal's movements; nothing of the target signal is fed into the compensatory loop, and the error is identical to the target ($H_{f_t,e}(j\omega) = 1$). Fig. 5(e) shows that low-gain pursuit control behavior (e.g., $K_f = 0.4$) yields relatively low errors for high-bandwidth target signals (e.g., 4 rad/s), much lower in fact than for any of the crossover-regressed compensatory-only control strategies in Fig. 5(d). An additional benefit of reducing K_f is that the error response $H_o^{\text{cmp}}(j\omega)$ can remain intact to suppress external disturbances (or remnant).

In preview tasks, HCs can respond to the trajectory ahead, as reflected in the model by the look-ahead time τ_f and smoothing time-constant $T_{l,f}$ parameters. Fig. 5(c) shows that nonzero values of τ_f and $T_{l,f}$ help to suppress tracking errors at all frequencies below approximately 6 rad/s. The error-amplification peak disappears completely when τ_f and $T_{l,f}$ are sufficiently high (≈ 1 s). This suggests that no reduced-gain control strategy is required to optimally track high-bandwidth target signals in preview tasks.

D. Predicting HC Behavior Adaptation

1) Approach: To predict how HCs adapt their behavior to the target signal bandwidth, the model in Fig. 4 is used to compute the tracking error, according to (2). The variance of the tracking error σ_e^2 is then minimized with a Nelder–Mead simplex method, similar as in [9], with 100 random parameter vector initializations to reasonably guarantee that the global optimum is found. The free model parameters in the optimization are $K_{e^\star}$, $T_{L,e^\star}$, K_f, $T_{l,f}$, and τ_f, as these capture the most relevant HC adaptations; other model parameters are set at fixed values. Closed-loop stability is enforced by constraining the target-tracking and disturbance-rejection phase margins, $\phi_m > 20^\circ$. A limit crossover frequency of $\omega_c > 0.5$ rad/s is selected to avoid a zero-output control strategy, and the maximum lead generation is limited to a typical value observed in HCs, namely $T_{L,e^\star} < 3$ s [2], [11], [12].

2) Settings: Predictions are made for seven target signal bandwidths (0.4–7.5 rad/s), two CE dynamics (single integrator, $\frac{1.5}{j\omega}$, and double integrator $\frac{5}{(j\omega)^2}$), and five display "cases" (compensatory, pursuit, and limited (2) and full preview). In single integrator tasks $T_{L,e^\star} = T_{l,e^\star} = 0$ and in double integrator tasks $T_{L,e^\star} \neq 0$ and $T_{l,e^\star} = 0$, to obtain typical linear equalization behavior [2], [8]. Predictions of compensatory behavior are made by setting $K_f = 1$, and $T_{l,f} = \tau_f = 0$ s, and optimizing for $K_{e^\star}$ and $T_{L,e^\star}$; for pursuit, K_f is additionally left as free parameter, and for preview, $T_{l,f}$ and τ_f are also free. Predictions for tasks with limited preview are obtained by restricting $\tau_f < \tau_p$ and $T_{l,f} < \tau_p$ [9]. The chosen preview times τ_p are approximately evenly distributed between 0 s (pursuit) and the "critical" time which yields "full" preview behavior [9], leading to 0.2 and 0.4 s in the single-integrator task, and 0.3 and 0.6 s in the double-integrator task. Full preview behavior is approximated by a preview time of 2 s, well beyond reported critical preview times [9]. The HC's physical limitation parameters are assumed to remain constant, with τ_v, ω_{nms}, and ζ_{nms} fixed at representative values of 0.2 s, 12 rad/s, and 0.2 (single integrator) and 0.28 s, 8.5 rad/s, and 0.45 (double integrator), respectively [9].

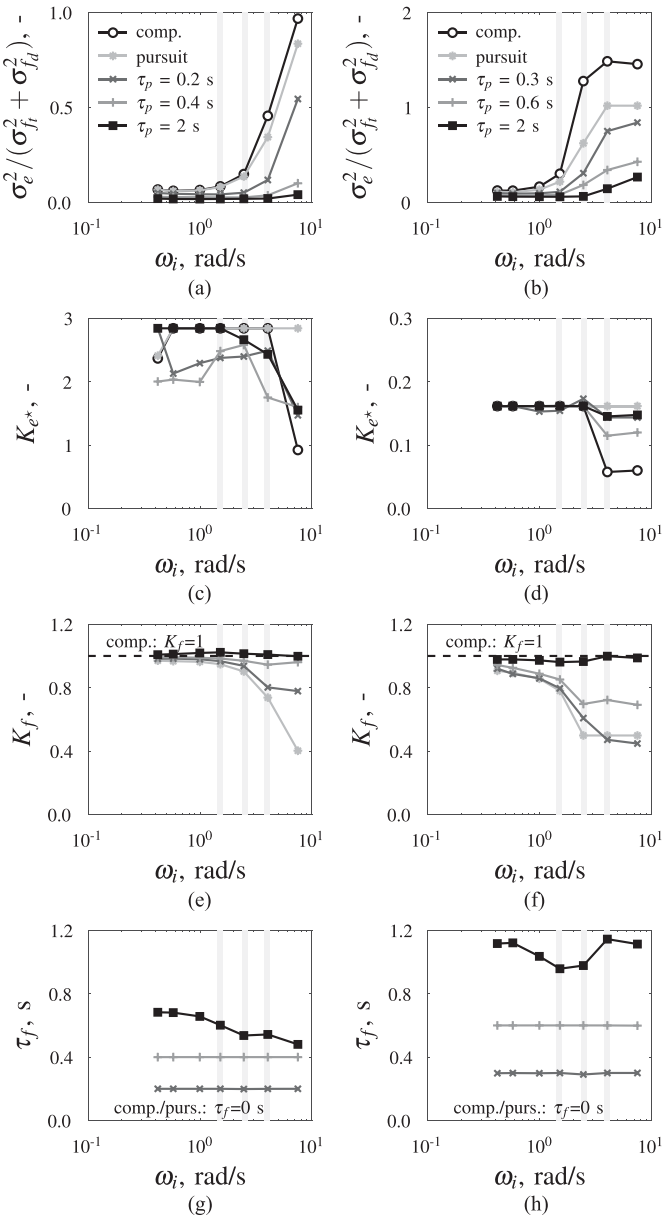

Fig. 6. Optimized performance (a, b) and corresponding model parameters (c–h) for single- (a, c, e, g) and double-integrator (b, d, f, h) CE dynamics.

The simulated target signals ($\sigma_{f_t}^2 = 1.61$ cm^2) are the sum of ten sinusoids, see (1), and differ only in the individual sinusoids' amplitudes. The seven signals have either 3, 4, 5, 6, 7, 8, or 9 low-frequency high-amplitude sinusoids, augmented with low-amplitude sinusoids at the remaining, higher frequencies beyond the input bandwidth ω_i. The three signals with 6, 7, and 8 low-frequency, high-amplitude sinusoids correspond to the 1.5, 2.5, and 4 rad/s bandwidth signals in Fig. 3. The disturbance signal is the sum of ten sinusoids with a 1.5 rad/s bandwidth, and its power $\sigma_{f_d}^2 = 0.26$ cm^2 is scaled to obtain predominantly a *target-tracking* task. The same disturbance signal is always used and no remnant is included, so $n(t) = 0$.

3) Results: Fig. 6(a) and (b) show that the maximum attainable performance deteriorates with higher-bandwidth target signals for all five simulation cases. However, performance

decreases markedly less with pursuit control as compared to compensatory control. Full preview yields the best performance, which is almost invariant with the target signal bandwidth. In compensatory tracking, a reduced-gain $K_{e^\star}$ strategy is beneficial at bandwidths higher than 4 rad/s in single-integrator tasks [see Fig. 6(c)], and 2.5 rad/s in double-integrator tasks [Fig. 6(d)], which corresponds well with previous experimental results [10], [11]. In pursuit, optimal tracking of higher-bandwidth target signals requires a constant error-response gain $K_{e^\star}$, and, instead, an attenuated target response [lower K_f at high frequencies in Fig. 6(e), (f)]. However, when more preview becomes available, a higher target response gain K_f (closer to 1) is beneficial, especially in higher-bandwidth tasks. In fact, with full preview, only minor behavior adaptations are required to optimally follow target signals with different bandwidths, as indicated by the approximately constant values of K_f and τ_f in Fig. 6(e)–(h). The optimal lead time-constant $T_{L,e^\star}$ and target smoothing time-constant $T_{l,f}$ are approximately invariant with bandwidth changes and are shown later in this article, together with the experimental results in Section V.

IV. Experimental Validation: Method

A. Hypotheses

First, corresponding to the offline model predictions, we hypothesize the following:

H.I: Task performance decreases when tracking higher-bandwidth target signals, independent of the experimental display. However, performance decreases slower when using pursuit as compared to compensatory displays, and even slower when preview is available.

Second, to confirm previous experimental results from compensatory tracking tasks [10], [11], we hypothesize the following:

H.II: In compensatory tasks, HCs first increase their control gains with increasing bandwidth of the target signal, in order to maintain a crossover frequency well above the input bandwidth. When a further increase in crossover frequency leads to instability, increased target signal bandwidths instead evoke crossover regression.

Third, based on the model predictions, we hypothesize that HCs adapt their behavior to increasingly high-bandwidth target signals in pursuit and preview tracking as follows:

H.III: In pursuit tasks, HCs attenuate their target response (lower K_f) and keep their error response constant ($K_{e^\star}$ and $T_{L,e^\star}$ invariant).

H.IV: In preview tasks, HC behavior is roughly invariant with changes in ω_i; the control gains remain constant ($K_{e^\star}$, $T_{L,e^\star}$, and K_f), while slight adaptations of τ_f and $T_{l,f}$ may occur to emphasize error-suppression at frequencies of the additional high-amplitude sinusoids.

B. Experiment Design

To test these hypotheses and verify the offline model predictions, an experiment was performed in the fixed-base simulator in the Human–Machine Interaction Laboratory at TU Delft. Participants were seated directly in front of the display screen and gave control inputs with a side-stick at their right-hand side, which was configured to only rotate around its roll axis. The experimental setup was equal to other recent preview tracking experiments, see [7]–[9] for details.

1) Independent Variables: Only a selection of the simulated task variable variations (see Section III) was experimentally tested, to avoid excessive measurement times. Double integrator CE dynamics were used throughout the experiment, as the predicted control behavior adaptation trends are largely identical, but more pronounced, as compared to single integrator tasks (see Fig. 6). Compensatory, pursuit, and preview ($\tau_p = 2$ s) display configurations were tested; their layouts corresponded to Fig. 2. The tested target signal bandwidths were 1.5, 2.5, and 4 rad/s and the power was 1.61 cm^2, identical to the signals tested by McRuer *et al.* [10] in compensatory tasks [see Fig. 3(a)]. The disturbance signal was held constant and was identical to that used in the simulations (1.5 rad/s bandwidth, 0.26 cm^2 power). The phases of the target and disturbance signals were generated randomly, but excessively low and high crest factors were avoided according to the method by Damveld *et al.* [18]. To avoid participants from memorizing parts of the target signal after repeated exposure, five different phase realizations were used. The experiment comprised the full factorial of the two independent variables (display and target bandwidth), yielding nine conditions in total.

2) Participants, Instructions, and Procedure: Nine volunteers participated in the experiment, all students of TU Delft. Participants signed for informed consent prior to the experiment and were instructed to minimize the tracking error, of which the rms value was reported after every measurement run. A single run lasted 128 s, of which the last 120 s were used for analysis and the first 8 s were used as run-in time. The experiment started with a familiarization phase, during which a single run was performed of each condition. The measurement conditions were then performed in an order randomized according to a balanced Latin-square. A single condition was repeated until performance and control activity were stable in five runs, which were then used for analysis. Participants performed four conditions on a first day, and returned on a second day for the remaining five conditions. The full experiment took around 5 h.

C. Analysis Approach

1) Dependent Measures: The variance of the error σ_e^2, the open-loop crossover frequency ω_c and phase margin ϕ_m, and the target-to-error dynamics $H_{f_t,e}(j\omega)$ were used as measures for tracking performance. Estimates of the prefilter dynamics $H_{o_f}(j\omega)$, the equalization dynamics $H_o^{\text{cmp}}(j\omega)$, and the HC model parameters were used to quantify participants' control behavior; see Section III for the definition of these measures.

2) Data Analysis: The calculation of the dependent measures from experimental data is identical to [7]–[9] and is repeated here only briefly for completeness. The error variance was obtained by computing the power-spectral density function of the error, and then integrating over the target, disturbance, or remnant input frequencies. The crossover frequencies and

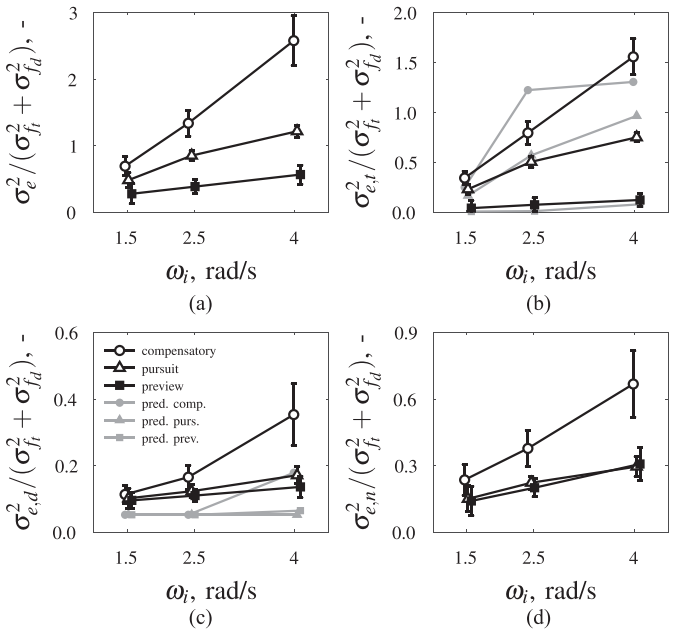

Fig. 7. Variance of the total tracking error (a) and contributions due to the target (b), disturbance (c) and remnant inputs (d); average over nine participants and 95% confidence intervals.

TABLE I
ANOVA RESULTS ON THE EFFECTS OF TARGET BANDWIDTH, THE $*$ SYMBOL INDICATES SIGNIFICANCE ($p < .0167$) AND ϵ IS THE CORRECTION ON THE DEGREES OF FREEDOM (2,16) FOR VIOLATIONS OF SPHERICITY

	compensatory			pursuit			preview		
	ε	F	sig.	ε	F	sig.	ε	F	sig.
σ_e^2	.57	77.2	$*$	1	123.1	$*$	1	28.9	$*$
$\sigma_{e,t}^2$	.62	135.3	$*$	1	165.5	$*$	1	42.1	$*$
$\sigma_{e,d}^2$	.57	22.9	$*$	1	30.2	$*$	1	9.1	$*$
$\sigma_{e,n}^2$	.61	19.8	$*$	.56	12.6	$*$	1	19.5	$*$
$\omega_{c,t}$	1	48.5	$*$	1	21.9	$*$	1	1.0	-
$\phi_{m,t}$	1	10.4	$*$	.52	32.2	$*$	1	1.9	-
$\omega_{c,d}$	1	48.5	$*$	1	15.1	$*$	1	1.1	-
$\phi_{m,d}$	1	10.4	$*$	.53	20.9	$*$	1	0.3	-
$K_{e^\star}$	.60	14.7	$*$	1	1.4	-	.58	1.2	-
τ_v	.55	10.3	$*$	1	19.9	$*$	1	1.6	-
$T_{L,e^\star}$	1	26.7	$*$	1	0.4	-	1	0.5	-
K_f				1	81.3	$*$	1	0.9	-
τ_f							1	0.7	-
$T_{l,f}$							1	0.8	-
ω_{nm}	1	5.5	$*$	1	8.3	$*$	1	0.3	-
ζ_{nm}	1	4.0	-	1	17.1	$*$	1	0.3	-

phase margins were obtained from estimates of the target and disturbance open-loop dynamics. Nonparametric estimates of the $H_{o_f}(j\omega)$ and $H_o^{\text{cmp}}(j\omega)$ dynamics were obtained using a multiloop system identification technique based on Fourier coefficients [19], [26], using the target and disturbance signals as instrumental variables. Model parameters were obtained with a least-squares approach, where the difference between the Fourier transforms of the measured and modeled control outputs, $U(j\omega)$ and $\hat{U}(j\omega)$, was minimized. From Fig. 4, it follows that $\hat{U}(j\omega) = H_o^{\text{cmp}}(j\omega)[H_{o_f}(j\omega)F_t(j\omega) - X(j\omega)]$. The global optimum was determined using a Nelder–Mead simplex algorithm, repeated 100 times with random initializations.

Repeated-measures ANOVA tests were performed on each dependent measure. As the effect of target bandwidth was our primary interest, a separate one-way ANOVA was performed for each display type, leading to three tests for each dependent measure. A Bonferroni correction was applied to the significance level ($p = 0.05/3$) and a Greenhouse–Geisser correction was applied when sphericity was violated. Unless otherwise noted, all errorbars in the next section reflect 95% confidence intervals. The intervals were corrected for between-participant variability to emphasize within-participant effects, by correcting each participant's mean of the specific measure to the mean across all participants (grand mean).

V. EXPERIMENTAL VALIDATION: RESULTS

A. Tracking Performance

1) Error Variance: Fig. 7(a) shows that a higher target signal bandwidth leads to worse total tracking performance (i.e., higher σ_e^2), regardless of the display (significant effects, see Table I). Performance deteriorates much more in compensatory tasks than in pursuit tasks, and more in pursuit tasks than in preview tasks, which corresponds well with the offline predictions. The target, disturbance, and remnant frequencies all contribute significantly to the performance reduction (see Fig. 7(b)–(d) and Table I), so both target-tracking and disturbance-rejection performance are worse, while errors due to remnant also increase. Note from Fig. 7(b) that the measured target-tracking performance in pursuit and preview tasks, the key focus of this article, was accurately predicted offline.

2) Target-to-Error Dynamics: Fig. 8 shows the estimated target-to-error dynamics. In compensatory tasks, higher bandwidths lead to a lower, but wider, error-amplification peak, while error suppression deteriorates at low frequencies. These effects correspond well to the reduced-gain $K_{e^\star}$ control strategy that was predicted in Fig. 5(a). In pursuit tasks, the target-to-error amplification peak also reduces with higher bandwidths. However, contrary to compensatory tasks, the peak's width does not increase, which corresponds well to the effects of a reduced target-response gain K_f, see Fig. 5(b). In preview tasks, no error-amplification peak is visible for any target signal bandwidth, which suggests that participants responded to the trajectory *ahead* [nonzero τ_f and $T_{l,f}$, Fig. 5(c)]. Errors due to the additional sinusoids at 2.5 and 4 rad/s are suppressed slightly better in higher-bandwidth preview tasks.

3) Crossover Frequency and Phase Margin: Fig. 9 shows the crossover frequencies ω_c and phase margins ϕ_m. In compensatory tasks, higher bandwidths result in a significantly lower *target* crossover frequency $\omega_{c,t}$ Fig. 9(a) and, especially at 2.5 rad/s, a higher phase margin $\phi_{m,t}$ Fig. 9(b), corresponding to a reduced-gain and more stable control strategy [2], [11]. In fact, in 2.5 and 4 rad/s bandwidth tasks, $\omega_{c,t} < \omega_i$, which indicates crossover regression. The target crossover frequency $\omega_{c,t}$ is around 2.5 rad/s for the lowest two bandwidths; comparable experiments have reported substantially higher values ($\approx$ 3.5 rad/s) [2], [11], [12], possibly because no disturbance signal f_d was included in those experiments [14]. Note that the

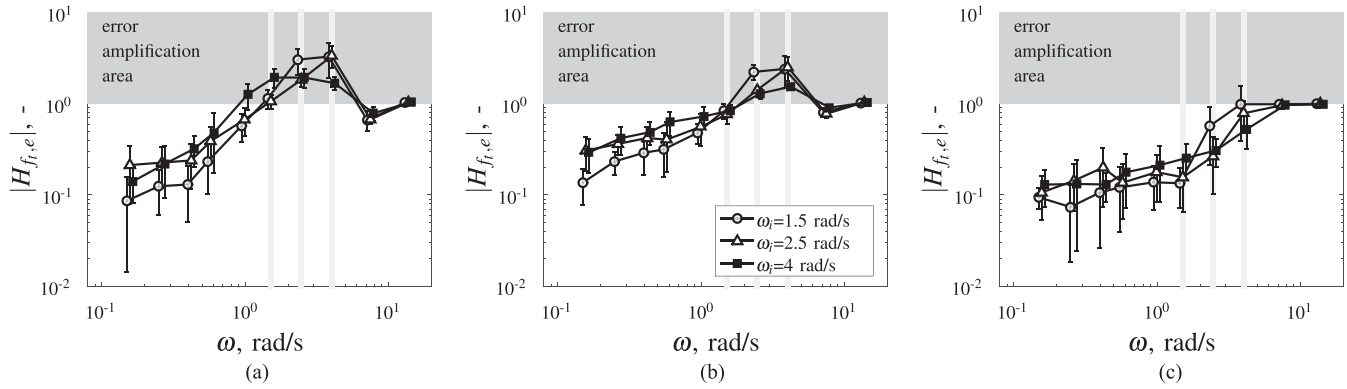

Fig. 8. Target-to-error dynamics, average over nine participants and standard deviations. Results are shifted slightly horizontally to reduce overlap. (a) compensatory. (b) pursuit. (c) preview.

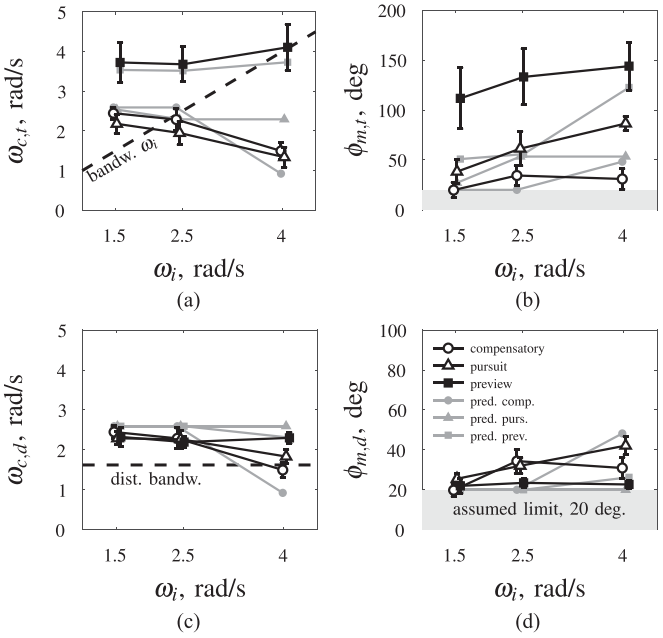

Fig. 9. Target crossover frequency (a) and phase margin (b), and disturbance crossover frequency (c) and phase margin (d); average over nine participants and 95% confidence intervals.

disturbance open-loop equals the target open-loop in compensatory tasks, so $\omega_{c,t} = \omega_{c,d}$ and $\phi_{m,t} = \phi_{m,d}$.

In pursuit tasks, the target crossover frequency $\omega_{c,t}$ also reduces with increasing bandwidth, see Fig. 9(a) (significant effect, see Table I). $\omega_{c,t}$ is approximately 0.2 rad/s lower and the phase margin $\phi_{m,t}$ is 20–60° higher as compared to compensatory tasks, suggesting that participants adopted a more conservative and stable control strategy. The disturbance crossover frequency $\omega_{c,d}$ also decreases with increasing target bandwidth, which contradicts the invariance predicted offline [gray triangles in Fig. 9(c)]. However, the measured decrease in $\omega_{c,d}$ is smaller than in compensatory tasks, which is especially clear at $\omega_i = 4$ rad/s.

In preview tracking tasks, the target crossover frequency $\omega_{c,t}$ is around 4 rad/s for all input bandwidths, see Fig. 9(a); Table I confirms that there is no significant effect. All frequencies below the input bandwidth ω_i are thus always tracked well, corresponding to Fig. 8(c). Additionally, the target phase margin $\phi_{m,t}$ is very high [100°–150°, Fig. 9(b)] due to the phase lead generated by responding to the trajectory ahead [8]. Contrary to compensatory and pursuit tasks, the disturbance crossover frequency $\omega_{c,d}$ and phase margin $\phi_{m,d}$ are approximately equal with all three input bandwidths, see Fig. 9(c) and (d) (no significant effects).

B. Human Control Behavior

Fig. 10 shows the estimated model parameters. In compensatory tasks, participants adapt their behavior from 1.5 to 2.5 rad/s tasks by reducing their control gain $K_{e^\star}$ [Fig. 10(a)], and increasing their lead time constant $T_{L,e^\star}$ [Fig. 10(c)], both by a factor of around two. As a result, $\omega_{c,t}$ remains almost equal while $\phi_{m,t}$ increases, which is indeed confirmed by Fig. 9(a) and (b). On the contrary, from 2.5 to 4 rad/s tasks, participants increase $K_{e^\star}$ (although only by approximately 25%), while again reducing $T_{L,e^\star}$ to the original value just above 1 s, which leads to clear crossover regression, see Fig. 9(a). Furthermore, participants adapt to higher bandwidths by reducing their time delay τ_v [Fig. 10(b), significant effect], increasing their neuromuscular break frequency ω_{nms} [Fig. 10(g), significant effect], and reducing the neuromuscular damping ζ_{nms} [Fig. 10(h), not significant].

In pursuit tasks, the response delay τ_v and neuromuscular damping ζ_{nms} decrease, while the neuromuscular break frequency ω_{nms} increases in higher-bandwidth tasks (all significant effects, see Table I), identical as in compensatory tasks. However, contrary to compensatory tasks, the error response gain $K_{e^\star}$ and lead time-constant $T_{L,e^\star}$ are roughly invariant, which is confirmed by the lack of significant effects, see Table I. The target response gain K_f decreases from around 0.75–0.5 Fig. 10(d). This adaptation corresponds well to the offline model predictions. These parameter adaptations, or invariants, are supported by the estimated HC control dynamics for pursuit tasks in Fig. 11. The "compensatory" control dynamics $H_o^{\text{cmp}}(j\omega)$ remain approximately constant, while the magnitude of the target prefilter $H_{o_f}(j\omega)$ decreases with increasing target bandwidth. The HC's actual feedforward dynamics lack the phase lead that is required for perfect target-tracking (gray line

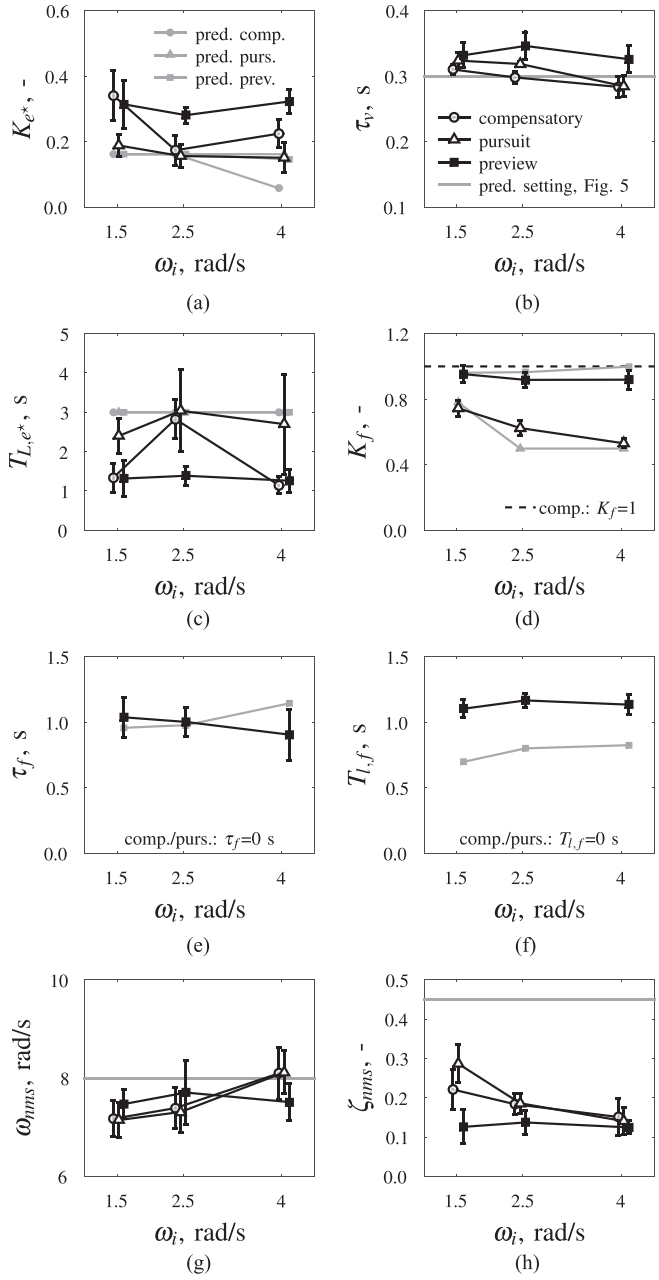

Fig. 10. Estimated model parameters, average over nine participants and 95% confidence intervals; indicated legends apply to all subfigures. (a) Error response gain. (b) Response delay. (c) Lead time-constant. (d) Target response gain. (e) Look-ahead time. (f) Target smoothing time-constant. (g) Neuromuscular break frequency. (h) Neuromuscular damping.

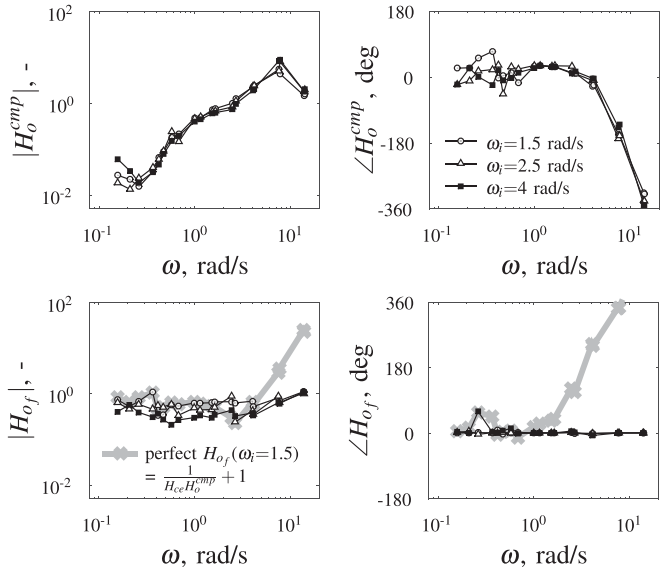

Fig. 11. Bode plot of estimated HC compensatory (H_o^{cmp}) and target prefilter dynamics (H_{o_f}) in the pursuit tasks. Data is of Participant 4, a representative participant for which the key behavior adaptation is clearly visible.

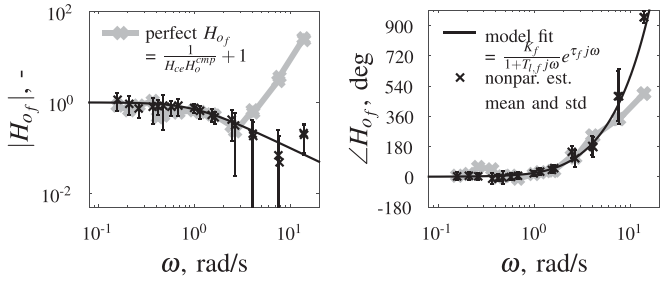

Fig. 12. Bode plot of estimated HC target prefilter dynamics H_{o_f} in the preview tasks with a 4 rad/s bandwidth target signal; Participant 4.

in Fig. 11), resulting in increasingly worse target tracking at higher frequencies. Exactly these frequencies are more strongly excited by higher-bandwidth target signals, which explains why HCs reduce their response gain K_f: to avoid amplifying these tracking errors.

In preview tasks, bandwidth changes yield only minor adaptations in the model parameters, and no significant effects are measured, see Fig. 10 and Table I. Interestingly, the average look-ahead time τ_f decreases slightly with bandwidth [from around 1.05–0.9 s, Fig. 10(e)], but with substantial between-participant variability, as indicated by the overlapping confidence intervals. The lower τ_f may not reflect a systematic adaptation to the bandwidth, but a more subtle adaptation to minimize the errors due to the additional high-amplitude sinusoids at 2.5 and 4 rad/s, see also Fig. 8(c). Nonetheless, the general way in which participants use the available preview for control is not affected by the target signal bandwidth, as the target response gain [$K_f \approx 0.95$, Fig. 10(d)] and lag time-constant [$T_{l,f} \approx 1.15$ s, Fig. 10(f)] are also approximately invariant. The estimated control dynamics in Fig. 12 show that the target trajectory is tracked almost perfectly at all frequencies below 4 rad/s, mostly because the phase lead due to τ_f allows for synchronizing the CE output with the target signal (as opposed to pursuit tasks, see Fig. 11, bottom right). Therefore, different-bandwidth target signals provide no incentive for HCs to strongly adapt their control behavior in preview tasks.

VI. Discussion

A. Hypotheses

The experimental data were presented to test four hypotheses regarding human adaptation to target signal bandwidth. Our first hypothesis (H.I) was that higher-bandwidth target signals lead

to reduced tracking performance, but relatively less so in pursuit and preview tasks. This hypothesis is certainly *confirmed*, which implies that preview displays should be favored over pursuit displays (and definitively over compensatory displays) in high-bandwidth target-tracking tasks. HCs in fact attain an error variance that is approximately *five times lower* with a preview display than with a compensatory display when tracking a 4 rad/s bandwidth target trajectory.

Corresponding to previous experiments [10]–[13], it was hypothesized (H.II) that *crossover regression* would occur in double-integrator compensatory tracking tasks with high-bandwidth target signals. This was indeed *confirmed*. However, regression occurred already with a relatively low-bandwidth target signal (2.5 rad/s), and not at 4 rad/s, as could be expected from the model predictions and most previous experiments [10]–[13]. Likely, this is a consequence of the relatively low overall crossover frequencies of our participants, which, according to the fourth "verbal adjustment rule" by McRuer and Jex [2], indeed leads to earlier crossover regression. Tentatively, participants adopted a comparably low crossover frequency as a result of the additional (but weak) disturbance signal in the current experiment, required for purposes of HC system identification.

In stark contrast to compensatory tracking tasks, HCs keep their error response almost constant when the target bandwidth is increased in *pursuit* tasks ($K_{e^\star}$ and $T_{L,e^\star}$ are only marginally adapted). HCs instead attenuate their target response (lower K_f), facilitated by the target marker that is visible on the pursuit display. Consequently, crossover regression occurs only in target-tracking, while stabilizing feedback control remains intact for disturbance-rejection. This *confirms* hypothesis H.III.

When *preview* is available, HCs can track the target trajectory almost perfectly up to relatively high frequencies of 4–6 rad/s, because they compensate for their own response delay simply by responding to the trajectory *ahead*. Therefore, there is no performance incentive that necessitates behavioral adaptations. Experiment participants indeed showed no signs of systematic adaptations to higher-bandwidth target signals. This *confirms* our fourth hypothesis (H.IV), and supports the invariant preview weighing reported for different bandwidth target signals by Jagacinski *et al.* [16].

B. Implications

This article is the final installment in a series of recent papers (i.e., [7]–[9]) that advanced the quasi-linear theory of manual control from compensatory tracking to more relevant pursuit and preview tracking tasks. The extension of the crossover-model theory to preview tracking [7] has now been experimentally validated for a fairly complete combination of key task variables. The model allows for predicting HC behavior in tracking tasks with: 1) gain, single- and double-integrator *CE dynamics* [8], 2) compensatory, pursuit, and preview *display configurations* and *preview times* of 0 (pursuit) to 2 s (full preview) [9], and 3) *target signal bandwidths* between 1.5 and 4 rad/s (this article). Further experimental validation of the theory for other task variable combinations nonetheless remains crucial. For example, the predicted HC adaptations to target bandwidth in tasks with single integrator CE dynamics have not been tested. Even more important, we still need to find the *limits of the theory* in capturing HC behavior, for example, in tasks with more complex CE dynamics and lower-bandwidth target signals (such as those encountered in real-life driving tasks).

Identical as in compensatory tracking tasks, the HC's *main* control mechanism in pursuit and preview tracking tasks is to minimize an error (although not the true error, but relative to the *prefiltered* "far-viewpoint"). This is the primary reason that a single, *unifying* model can capture HC behavior in these—relatively different—tracking tasks. Unfortunately, due to the available degrees in which HCs can adapt their behavior in preview tasks, it is not trivial to formulate a set of *verbal adjustment rules* that is equally comprehensive, yet simple, as done by McRuer *et al.* [2], [10] for compensatory tracking. As a first-order approximation, HCs adapt their main (far-viewpoint) response in preview tasks to optimize tracking performance *at low frequencies*, within their physical limitations. The perfect target-prefiltering dynamics in (4) reveal *how much* preview is required: the far-viewpoint should be positioned at that look-ahead time τ_f s ahead, where its associated phase lead equals the combined CE and HC response phase lag. At the higher frequencies of the target signal, which are often less relevant, HC adaptation appears not to be motivated by optimal performance alone, but also by factors such as control effort, experience and motivation. The near-viewpoint response, as modeled in [7], captures high-frequency target tracking behavior in preview tasks to some extent, but—at least for now—remains difficult to predict.

The basic quasi-linear theory of manual (preview) control that is now available could find even broader societal applications after two key innovations. First, the current models should be extended to capture HC behavior in a wider range of real-life control tasks. As a first step, we already adapted the quasi-linear preview model to capture driver steering on winding roads [27]. This extension explains how the near- and far-viewpoint preview responses relate to prevailing two-level theories of driver steering [27] (e.g., see Land and Horwood [28]). Second, as noted by Mulder *et al.* [1], the quasi-linear framework would benefit from an update to capture time-variations of the HC's behavior. The models can then be applied for *online* monitoring and adaptive (intelligent) support of HCs in manual control tasks, for example, in tomorrow's highly-automated road vehicles.

VII. Conclusion

This article investigated the effects of target trajectory bandwidth on manual control behavior in pursuit and preview tracking tasks. Offline analysis with a quasi-linear HC model accurately predicted human-in-the-loop measurements in double integrator tasks; similar predictions for single integrator tasks remain to be experimentally validated. Humans adapt to higher-bandwidth target trajectories in pursuit tasks mainly by reducing their *feedforward*, target response gain, as opposed to the adaptation of their *feedback* control behavior in compensatory tracking tasks. In preview tasks, human control behavior is largely invariant to target bandwidth variations between 1.5 and 4 rad/s. A single quantitative theory is now

available for human control behavior in all basic tracking tasks, including human adaptation to key task variables. The theory facilitates predictions for a wide range of display configurations, CE dynamics, preview times, and target signal bandwidths.

REFERENCES

[1] M. Mulder *et al.*, "Manual control cybernetics: State-of-the-art and current trends," *IEEE Trans. Human-Mach. Syst.*, vol. 48, no. 5, pp. 468–485, Oct. 2018.

[2] D. T. McRuer and H. R. Jex, "A review of quasi-linear pilot models," *IEEE Trans. Hum. Factors Electron.*, vol. HFE-8, no. 3, pp. 231–249, Sep. 1967.

[3] L. R. Young, "On adaptive manual control," *IEEE Trans. Man-Mach. Syst.*, vol. MMS-10, no. 4, pp. 292–331, Dec. 1969.

[4] R. J. Wasicko, D. T. McRuer, and R. E. Magdaleno, "Human pilot dynamic response in single-loop systems with compensatory and pursuit displays," Air Force Flight Dynamics Laboratory, Wright-Patterson Air Force Base, OH, Tech. Rep. AFFDL-TR-66-137, 1966.

[5] F. M. Drop, D. M. Pool, H. J. Damveld, M. M. van Paassen, and M. Mulder, "Identification of the feedforward component in manual control with predictable target signals," *IEEE Trans. Cybern.*, vol. 43, no. 6, pp. 1936–1949, Dec. 2013.

[6] V. A. Laurense, D. M. Pool, H. J. Damveld, M. M. van Paassen, and M. Mulder, "Effects of controlled element dynamics on human feedforward behavior in ramp-tracking tasks," *IEEE Trans. Cybern.*, vol. 45, no. 2, pp. 253–265, Feb. 2015.

[7] K. van der El, D. M. Pool, H. J. Damveld, M. M. van Paassen, and M. Mulder, "An empirical human controller model for preview tracking tasks," *IEEE Trans. Cybern.*, vol. 46, no. 11, pp. 2609–2621, Nov. 2016.

[8] K. van der El, D. M. Pool, M. M. van Paassen, and M. Mulder, "Effects of preview on human control behavior in tracking tasks with various controlled elements," *IEEE Trans. Cybern.*, vol. 48, no. 4, pp. 1242–1252, Apr. 2018.

[9] K. van der El, S. Padmos, D. M. Pool, M. M. van Paassen, and M. Mulder, "Effects of preview time in manual tracking tasks," *IEEE Trans. Human-Mach. Syst.*, vol. 48, no. 5, pp. 486–495, Oct. 2018.

[10] D. T. McRuer, D. Graham, E. S. Krendel, and W. J. Reisener, "Human pilot dynamics in compensatory systems, theory models and experiments with controlled element and forcing function variations," Air Force Flight Dynamics Laboratory, Tech. Rep. AFFDL-TR-65-15, 1965.

[11] G. C. Beerens, H. J. Damveld, M. Mulder, M. M. van Paassen, and J. C. van der Vaart, "Investigation into crossover regression in compensatory manual tracking tasks," *J. Guid., Control, Dyn.*, vol. 32, no. 5, pp. 1429–1445, Sep./Oct. 2009.

[12] H. G. H. Zollner, D. M. Pool, H. J. Damveld, M. M. van Paassen, and M. Mulder, "The effects of controlled element break frequency on pilot dynamics during compensatory target-following," in *Proc. AIAA Guid., Navig., Control Conf.*, Toronto, ON, Canada, Aug. 2010.

[13] H. Gerisch, G. Staude, W. Wolf, and G. Bauch, "A three-component model of the control error in manual tracking of continuous random signals," *Human Factors*, vol. 55, no. 5, pp. 985–1000, Oct. 2013.

[14] R. W. Allen and H. R. Jex, "An experimental investigation of compensatory and pursuit tracking displays with rate and acceleration control dynamics and a disturbance input," NASA, Tech. Rep. CR-1082, 1968.

[15] M. Tomizuka and D. E. Whitney, "The human operator in manual preview tracking (an experiment and its modeling via optimal control)," *J. Dyn. Sys., Meas., Control*, vol. 98, no. 4, pp. 407–413, Dec. 1976.

[16] R. J. Jagacinski, G. M. Hammond, and E. Rizzi, "Measuring memory and attention to preview in motion," *Human Factors*, vol. 59, no. 5, pp. 796–810, Aug. 2017.

[17] W. Mugge, D. A. Abbink, and C. Van der Helm, "Reduced power method: How to evoke low-bandwith behaviour while estimating full-bandwidth dynamics," in *Proc. 2007 IEEE 10th Int. Conf. Rehabil. Robot.*, Noordwijk, The Netherlands, Jun. 2007, pp. 575–581.

[18] H. J. Damveld, G. C. Beerens, M. M. van Paassen, and M. Mulder, "Design of forcing functions for the identification of human control behavior," *J. Guid., Control, Dyn.*, vol. 33, no. 4, pp. 1064–1081, 2010.

[19] R. L. Stapleford, D. T. McRuer, and R. E. Magdaleno, "Pilot describing function measurements in a multiloop task," *IEEE Trans. Hum. Factors Electron.*, vol. HFE-8, no. 2, pp. 113–125, Jun. 1967.

[20] R. W. Allen and H. R. Jex, "A simple Fourier analysis technique for measuring the dynamic response of manual control systems," *IEEE Trans. Syst., Man and Cybern.*, vol. SMC-2, no. 5, pp. 638–643, Sep. 1972.

[21] R. W. Pew, J. C. Duffendack, and L. K. Fensch, "Sine-wave tracking revisited," *IEEE Trans. Hum. Factors Electron.*, vol. HFE-8, no. 2, pp. 130–134, Jun. 1967.

[22] R. E. Magdaleno, H. R. Jex, and W. A. Johnson, "Tracking quasi-predictable displays subjective predictability gradations, pilot models for periodic and narrowband inputs," in *Proc. 5th Annu. NASA-Univ. Conf. Manual Control*, 1969, pp. 391–428.

[23] T. Yamashita, "Effects of sine wave combinations on the development of precognitive mode in pursuit tracking," *Quart. J. Exp. Psychol.*, vol. 42A, no. 4, pp. 791–810, 1990.

[24] F. M. Drop, R. J. de Vries, M. Mulder, and H. H. Bülthoff, "The predictability of a target signal affects manual feedforward control," in *Proc. 13th IFAC/IFIP/IFORS/IEA Symp. Anal., Des. Eval. Man-Mach. Syst.*, Kyoto, Japan, 2016.

[25] T. B. Sheridan, "Three models of preview control," *IEEE Trans. Hum. Factors Electron.*, vol. HFE-7, no. 2, pp. 91–102, Jun. 1966.

[26] M. M. van Paassen and M. Mulder, "Identification of human operator control behaviour in multiple-loop tracking tasks," in *Proc. 7th IFAC/IFIP/IFORS/IEA Symp. Anal., Des. Eval. Man-Mach. Syst.*, Kyoto, Japan, 1998, pp. 515–520.

[27] K. van der El, D. M. Pool, M. M. van Paassen, and M. Mulder, "A unifying theory of driver perception and steering control on straight and winding roads," *IEEE Trans. Human-Mach. Syst.*, to be published, doi: 10.1109/THMS.2019.2947551.

[28] M. F. Land and J. Horwood, "Which parts of the road guide steering?" *Nature*, vol. 377, pp. 339–340, Sep. 1995.